CHAPTER

9 A Digital Microfabrication-Based System for the Fabrication of Cancerous Tissue Models

Qudus Hamid,[1] Chengyang Wang,[1] Jessica Snyder,[1] Yu Zhao,[2] Wei Sun,[1,2,3]

[1]Department of Mechanical Engineering and Mechanics, Drexel University, Philadelphia, PA, USA; [2]Mechanical Engineering and Biomanufacturing Research Institute, Tsinghua University, Beijing, China; [3]Shenzhen Biomanufacturing Engineering Laboratory, Shenzhen, Guangdong, China

CONTENTS

INTRODUCTION

Micro-electro-mechanical systems (MEMS) technologies have been very attractive and have demonstrated the potential for many applications in the field of

Biofabrication.

tissue engineering, regenerative medicine, and life sciences. These fields bring together the multidisciplinary field of engineering and integrated sciences to fabricate tissue models that aid the exploration, generation, or regeneration of organic tissues and organs [1–3]. MEMS were first introduced on conventional semiconductor materials, which were used to develop integrated circuits (ICs). Since the development of the first IC with MEMS technologies, MEMS have been utilized in many other fields with great success. MEMS technology, however, is expensive and has many limitations [4–6].

There is an overwhelming need for substitutes to repair tissues and organs because of disease, trauma, or congenital problems. In the United States alone, as many as 20 million patients per year suffer from various organ- and tissue-related maladies caused by burns, skin ulcers, diabetes, and connective tissue defects, which include bone and cartilage damage. More than 8 million surgical procedures are performed annually to treat these cases, over 70,000 people are on transplant waiting lists, and an additional 100,000 patients die due to the lack of availability of appropriate organs [7]. Scientists are working around the clock to develop pharmaceuticals and tissue replacements that would allow humans to live longer lives. However, many of these developments require tremendous amounts of research on their effects on humans. Quite often, the use of animal and human models is limited by the feasibility of testing protocols, availability, and ethical anxieties [8,9]. The digital micro-mirroring microfabrication (DMM) system will give scientists the capabilities to develop models that can be utilized to characterize new pharmaceuticals and tissue replacements and to develop models to study fatal diseases such as cancers [10–12]. This biologically inspired microfabrication system has the potential to develop critical three-dimensional models for the investigation of various tissue models and biological sensors. Three-dimensional biological models are preferred for in vitro investigation, since these models eliminate the limitations of traditional mainstay two-dimensional models [13,14].

The DMM system can be used to fabricate many advantageous devices. Among them, microfluidics systems have the most tissue engineering, regenerative medicine, and life sciences applications to develop in vitro tissue models. Unlike many conventional microfabrication techniques and/or devices available to fabricate tissue models, this system eliminates the need for masks by incorporating a dynamic maskless fabrication technique [15–18]. Since the DMM system can develop models on a micro-scale level, this makes research more economic, requiring fewer reagents and fewer cells, and it will allow for consistency in experimental analysis to perform limited interactions with end users [19–21]. The DMM system is specifically designed for the development of biologically inspired devices, which include, but are not limited to, biosensors, Lindenmayer systems, and micro-organs (Figure 9.1). This fabrication system eliminates the limitations of conventional photolithography and gives the end user the ability to develop advantageous models [16,22].

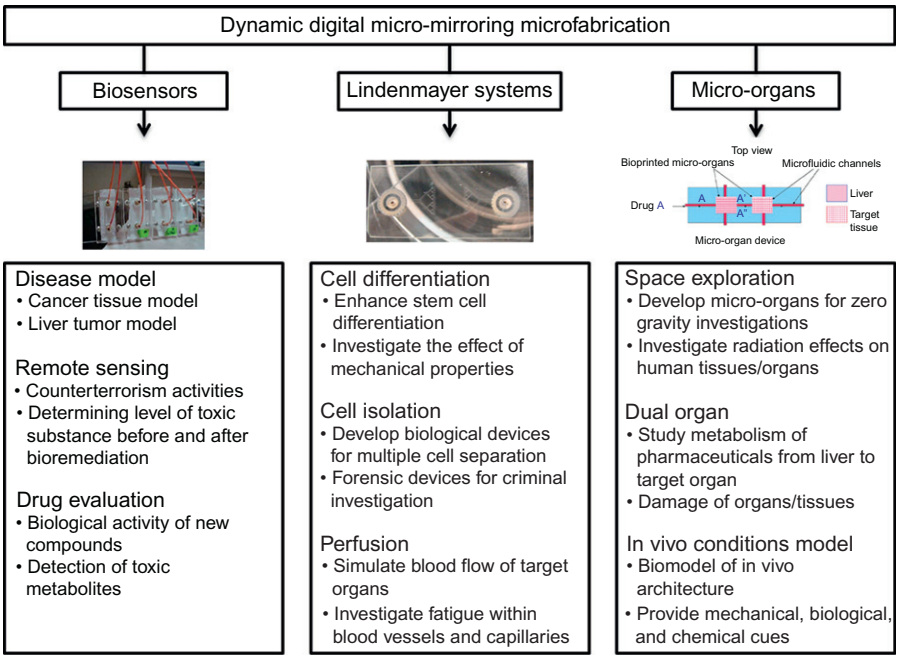

FIGURE 9.1

Applications of the dynamic digital micro-mirroring microfabrication system.

9.1 Digital micro-mirroring microfabrication system

The DMM system consists of three major components: a digital micro-mirroring projection system, a photolithographic substrate alignment system, and a mask modeling system. The micro-mirroring projection system is connected to a computer interface. The computer system activates and deactivates the projection of the mask onto the substrate. The photolithographic substrate alignment system consists of a digital microscopic device that allows for alignment of the substrate's features. The mask modeling system utilizes computer-aided design (CAD) technologies to design a mask for projection. The mask projected by the micro-mirrors must be in .jpeg, .bitmap, or .gif format. Figure 9.2 illustrates the digital micro-mirroring microfabrication system and its corresponding flow diagram.

9.1.1 Digital micro-mirroring projection system

The micro-mirroring projection system has the potential to switch between masks within a matter of microseconds, while offering high-resolution performance in spatial light modulation (SLM). With ultraviolet (UV) light, this system offers a

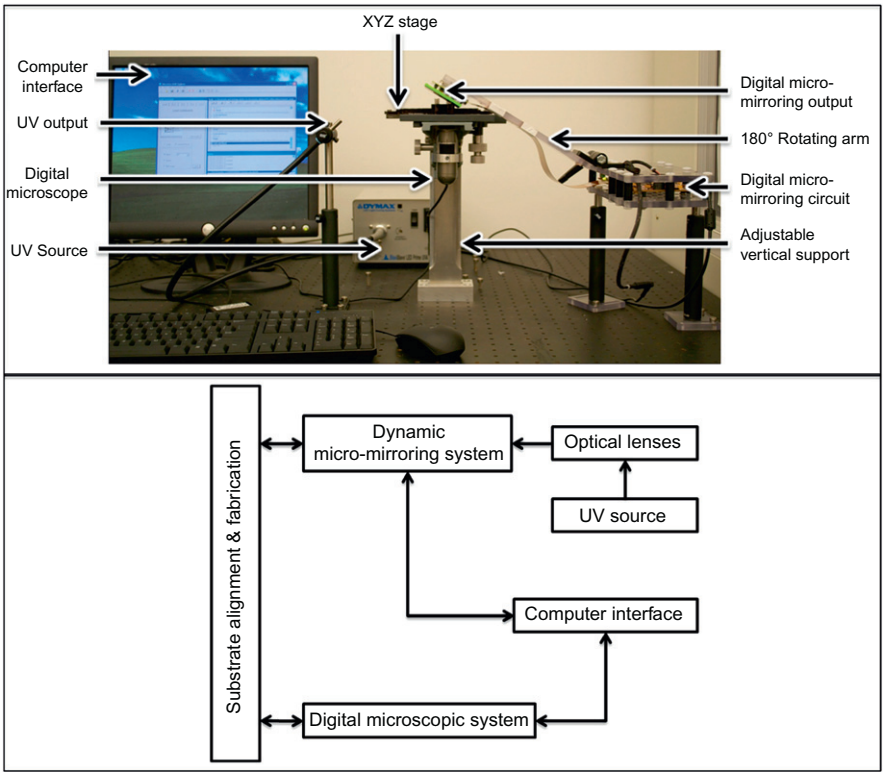

FIGURE 9.2

(Top) Digital micro-mirroring microfabrication system. (Bottom) Structure of the digital micro-mirroring microfabrication system.

flexible platform to design and develop proof of concepts, tissue models, biosensors, micro-organs, and Lindenmayer systems. The main component of the digital micro-mirroring projection system is the digital micro-mirror device (DMD), which is an optical semiconductor module that allows the digital manipulation and projection of UV light. The DMD is mounted directly above the alignment platform and is angled toward the UV light source. The DMD is completely adjustable in terms of elevation and angle. The UV light source emits an adjustable light in terms of intensity and exposure time. The light from the UV lamp travels and uniformly distributes on the micro-mirrors. Figure 9.3 shows the control system diagram of the digital micro-mirroring projection system and the direction of the light projected onto the micro-mirrors and their corresponding reflection. The DMD is comprised of millions of micro-mirrors aligned in rows and columns. During the projection phase, the DMD mirrors would be either on or off, depending on the pattern being projected. The DMD mirrors that are turned on would absorb the UV light and project it downward, while mirrors that are turned off would reflect the UV light in the opposite direction [23]. Energy is

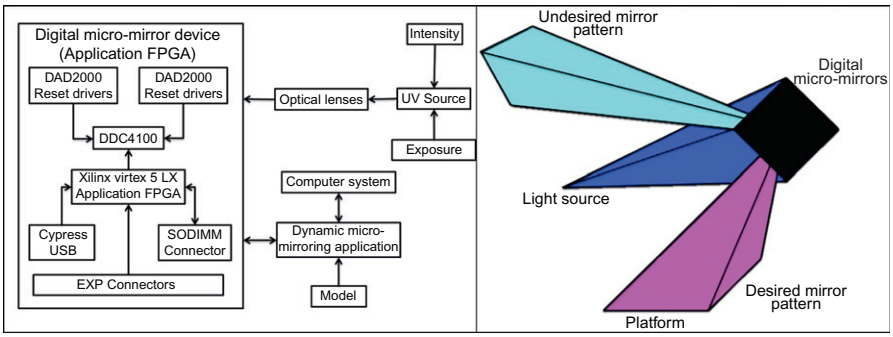

FIGURE 9.3

(Left) Structure of the digital micro-mirroring projection system. (Right) Illustration of light reflection on the digital mirrors.

lost during transmission of light from the UV source to the digital micro-mirror and from the micro-mirror to the substrate. The transmission wavelength of the system ranges from 370 nm to 410 nm, while the maximum energy output of the UV source is 15 MW at 100 percent intensity.

9.1.2 Photolithographic substrate alignment system

The photolithographic substrate alignment system consists of two actuators (manual): one that controls motion in the X direction (Cartesian coordinates) and one that controls motion in the Y direction (Cartesian coordinates). Together these two actuators span the X-Y plane of the alignment platform. Along with the X-Y actuators, there is a pair of fasteners that holds the substrate in place. Since this a microfabrication device, any small movement can be catastrophic. To ensure that the substrate's features are aligned with the projected mask (from the micro-mirror projection system), a digital microscopic device is directly below the alignment platform (centered) with a live feed to the computer system. This microscopic device features a fully adjustable magnification ranging from 20X to 200X. In addition to the magnification, the microscopic device has the capability to adjust its focal distance. The control structure of the photolithographic substrate alignment system is featured in Figure 9.4.

9.2 Multinozzle biologics deposition system

The multinozzle biologics deposition system is inspired by rapid prototyping technology and is built on the CAD/CAM platform, which is integrated with solid free-form automation to assemble biologics in three-dimensional space. This system consists of three motion arms for three-dimensional spatial control and a material deposition that houses up to 4 biological materials at once. The deposition system utilizes micro-valve nozzle systems that can deposit a wide range of

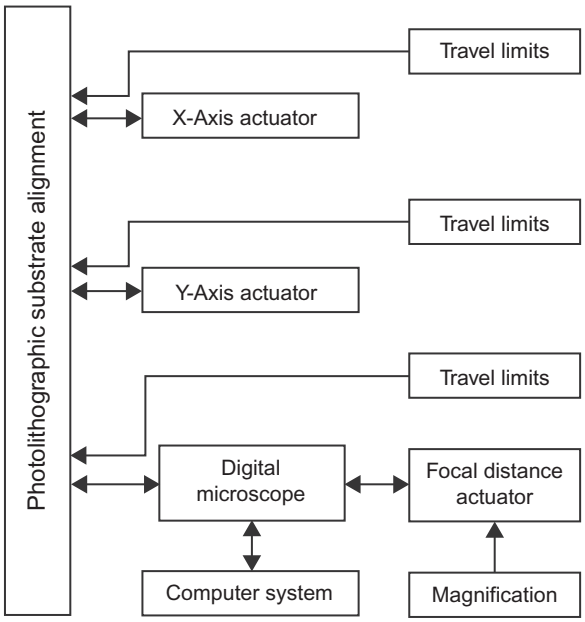

FIGURE 9.4

Structure of the photolithographic substrate alignment system.

solutions with a wide range of material and biological properties. This printer is fully integrated and computer controlled. The multinozzle biologics deposition system eliminates human error and provides its end users with precision control during fabrication procedures. This system executes micron-scale spatial control to generate cell-laden constructs. The multinozzle biologics deposition system is capable of depositing heterogeneous materials, cell types, and biological factors in a controlled and reproducible manner [24–26]. Cell printing is considered to be an effective biofabrication tool to assemble biologics. Figure 9.5 illustrates an overview of the multinozzle biologics deposition system configuration.

9.3 Methods and materials

The micro-fluidic chips are fabricated from two materials. Polydimethylsiloxane (PDMS) (Sigma-Aldrich, St. Louis, MO) is used as the basis for the chip, while SU-8 2100 (MicroChem Corp., Newton, MA) is used to fabricate the micro-architecture of the chip. We examine two biological explorations in this chapter. The first biological study is a preliminary investigation that characterized the fabricated chips in terms of the cell's ability to attach and proliferate in the micro-channels. The

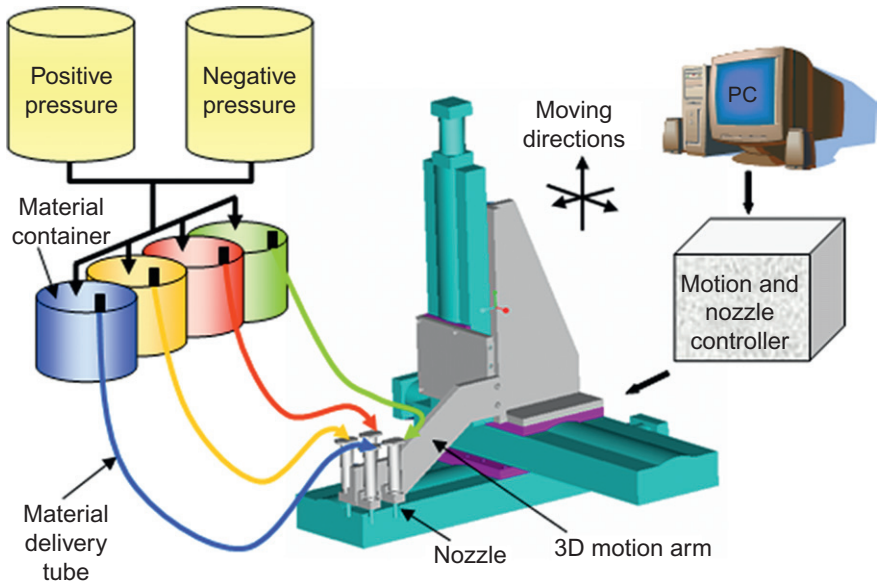

FIGURE 9.5

Overview of system configuration of 3D MDM system.

preliminary investigation used 7F2 cell line (mouse osteoblast), and the second biological investigation used MDA-MB-231 cell line (human breast cancer cells), both obtained from ATCC in Manassas, Virginia. The second cell line characterizes the model's potential to develop a cancerous model. (Unless listed otherwise, all cell culture supplements were obtained from ATCC.) All biological investigation data are expressed as the mean ± standard deviation for a sample size of 3 (n = 3).

9.3.1 Fabrication protocols and cell cultures

The enclosure of the chip is fabricated first. The enclosure has a platform (bottom) and a lid (top). The entire enclosure is fabricated from PDMS. The input and output ports are a nylon-based Luer-lock port (McMaster-Carr, Robbinsville, NJ). PDMS is mixed at 1:15 ratio, degassed, and cured in an aluminum mold at 130°C for 10 minutes. Cured PDMS is cooled and removed from the aluminum mold. This process is repeated for the lid, and the Luer-lock ports are placed in position prior to being cured on the hotplate. Figure 9.6 shows a model of the PDMS enclosure.

SU-8 is poured and leveled in the PDMS slot (bottom of the enclosure). It is then soft-baked at 65°C for 20 minutes, and then at 90°C for 220 minutes for stability. It is cooled for 30 minutes and then exposed at the recommended exposure time (this is based on the amount of energy required for crosslinking): DMM

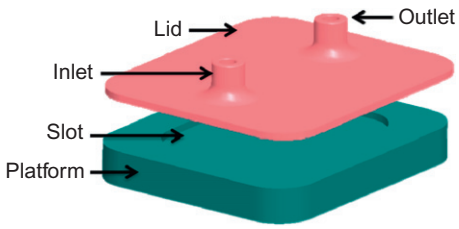

FIGURE 9.6

Model of the PDMS enclosure.

exposure time is 10.75 minutes, 265 mJ. The exposed sample is then hard-baked at 65°C for 15 minutes, and then at 90°C for 30 minutes for structural integrity. The sample is cooled for another 30 minutes and then developed with SU-8 Developer (MicroChem Corp., Newton, MA). During this stage, the unwanted material will be washed away. Development time is 8 to 15 minutes. Once developed, the sample is removed and rinsed with DI water to remove any excess materials in the channel. All samples used for biological investigations are sterilized first by dry heat of 150°C and then autoclaved. This rigorous process is used to ensure that the samples are completely sterile. Prior to cell deposition in the micro-channels, all samples are plasma treated with a Harrick Plasma Treater (Harrick Plasma, Ithaca, NY). Each sample was vacuumed to a pressure of 100 mTorr to 1 Torr, and the plasma was treated at high RF power settings for 120 seconds. Plasma treatment is used to created a seal between enclosures and to enhance cell attachment and proliferation with the SU-8 channels.

The DMM utilizes a systematic approach to fabricate models using a photosensitive polymer. The digital micro-mirroring microfabrication system projects an image of the desired structure onto the photosensitive polymer. Once the polymer is exposed, it manipulates the material's chemical properties and mimics the projected pattern [27]. Once exposed, the samples will undergo baking, developing, and sterilization processes (as previously detailed). Figure 9.7(a) shows the model of the microfluidic pattern, (b) the fabricated microfluidic pattern on the chip (bottom enclosure), and (c) a microscopic view of the channels in the chip.

7F2 and MDA-MB-231 cell lines have similar cell culture protocols. Both cell lines were seeded onto 75 cm^2 vented flasks and incubated. Six hours after the cells were seeded, the culture medium (cell depended) was changed to remove any dead cells in the flask; the culture medium was also changed every 2 to 3 days until the flasks were confluent. Confluent flasks were harvested and counted using a hemocytometer. The cells were then centrifuged again, in which the cell pallet was suspended to a cell density of 1×10^6 cells/mL. The cells were then loaded into the printer, where they were printed into the micro-channels (Figure 9.8). After the printing process, the chip would be sealed (sealing is possible to plasma treatment) with a PDMS lid, which has one input and one output. Culture media were changed

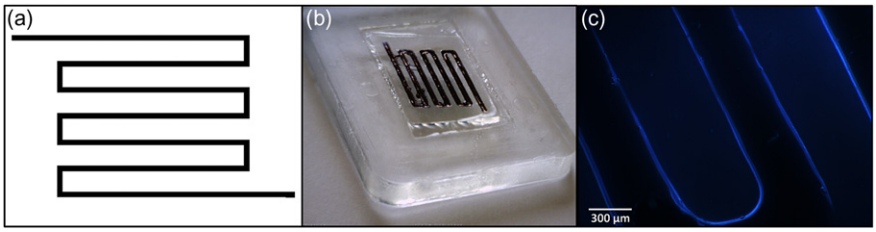

FIGURE 9.7

(a) Modeled microfluidic pattern. (b) Fabricated microfluidic pattern. (c) Microscopic view of the channel.

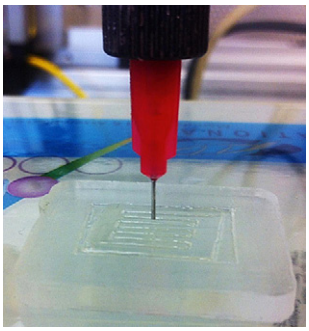

FIGURE 9.8

Close-up view of cells being printing into the micro-channels.

every 2 to 3 days and after every characterization point. 7F2 cells were incubated at 37°C with 95 percent air and 5 percent CO_2, while MDA-MB-231 cells were incubated at 37°C with 100 percent air.

9.4 Results

9.4.1 Preliminary investigation

The micro-channel array fabricated for this investigation is a single-layered open chip. An open chip study characterizes the feasibilities of the chip's potential for cell attachment and proliferation. The open chip study does not have a lid; cells are seeded into the micro-channels using the cell printer and then placed in the incubator for characterization. The two sample types for this preliminary investigation are nonplasma-treated micro-channels and plasma-treated micro-channels. Plasma treatment of the micro-channels enhances the surface properties. The chips fabricated for this investigation are the ones shown in Figure 9.7.

9.4.1.1 Cell interaction

It is important that the cells maintain interaction in the micro-channels; without the cell–cell interaction, cells cannot proliferate and differentiate into mature cells that are essential for functional tissues. A fluorometric indicator (Alamar Blue, Serotec) of cell metabolic activity was utilized to determine the cell proliferation in the channels [28–30]. Cell-laden samples (both treated and untreated) were removed from the culture plates, washed twice, placed in a new culture plate where 10 percent (v/v) Alamar Blue was added to the micro-channels, and incubated for 4 hours. The resulting solution was removed from the culture plate and placed in the microplate reader (GENios, TECAN, North Carolina) whose excitation and emission wavelengths were 535 nm and 590 nm, respectively. This study was conducted on days 0, 3, 5, 7, 10, and 14. The results of this study are shown in Figure 9.9, where the untreated samples showed no upregulation of cell proliferation. However, the plasma-treated samples showed a linear progression of proliferation up to day 7. After day 7, this progression subdued. The decline of proliferation of the plasma-treated samples on day 7 is believed to be due to limited space for cells to continue to grow in the micro-channels. Figure 9.10 is

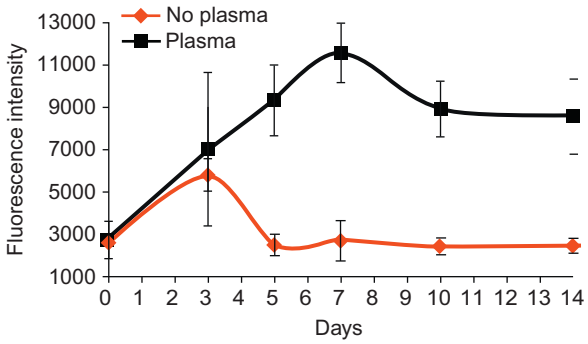

FIGURE 9.9

Cell proliferation on treated and untreated microfluidic constructs.

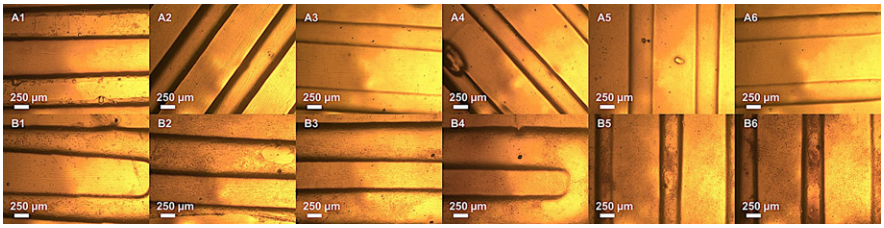

FIGURE 9.10

An optical snapshot of cells growing in the microfluidic chips on days 0, 3, 5, 7, 10, and 14 for untreated (A1–A6) and treated (B1–B6) samples.

an optical snapshot of cells growing in the microfluidic chips on days 0, 3, 5, 7, 10, and 14 for untreated (A1–A6) and treated (B1–B6) samples.

9.4.1.2 Cytotoxicity analysis

The MarkerGene™ Live:Dead/Cytoxicity Assay Kit (Marker Gene Technologies, Inc.; published by Marker Gene Technologies, Inc., Eugene, OR) was used to analyze the cytotoxicity of the plasma- and nonplasma-treated chips. Manufacturers' protocols were followed to create the working live:dead solution from the propidium iodide (PI) solution and the carboxyfluorescein di-acetate (CFDA) solution. The carboxyfluorescein dye is retained in live cells, producing a green fluorescence, while cells with damaged membranes allow the entrance of PI, which undergoes a fluorescence enhancement upon binding to nucleic acids, promoting a red fluorescence in dead cells. Qualitative and quantitative data were collected from the microfluidic cell-laden constructs on days 7 and 14 after cells were printed into the micro-channels. Figure 9.11 illustrates live (green) and dead (red) cells in the micro-channels of the construct. Images A1 and A2 in Figure 9.11 show the live and dead cells in the nonplasma-treated sample, while B1 and B2 show the live and dead cells in the plasma-treated micro-channels on days 7 and 14, respectively. On day 7, there were more living cells on the plasma-treated sample compared with day 14. Additionally, the plasma-treated samples show that its enhanced surface properties have the capability to support cell attachment and proliferation in the micro-channels.

9.4.2 Cancer model investigation

The preliminary investigation showed that chips fabricated with the DMM system have the potential to develop micro-tissue models. This investigation will move one step further and characterize the chip's ability to develop a cancer model. The chips used in this investigation are fully developed chips with a sealed

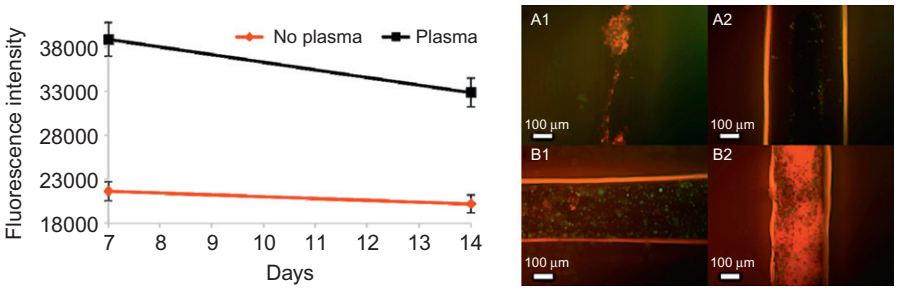

FIGURE 9.11

(Left) Quantitative results of live cells in the treated and untreated samples on days 7 and 14. (Right) Fluorescence images of cells in the channels of untreated (A1–A2) and treated (B1–B2) samples on days 7 and 14, respectively.

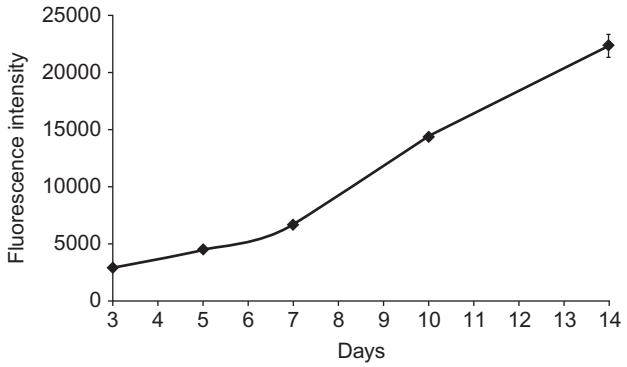

FIGURE 9.12

Cell proliferation of MDA-MB-231 cells in the micro-channels.

enclosure with one input and one output. All samples are plasma treated. The cells are printed into the micro-channels using the cell printer and are sealed immediately after printing is concluded. Culture medium is fed through the inlet of the chip according to the culture procedures discussed earlier in the chapter.

9.4.2.1 Cell interaction

A fluorometric indicator (Alamar Blue, Serotec) of cell metabolic activity was utilized to determine the cell proliferation in the channels. Cell-laden samples were sectioned, washed twice, and placed into a culture plate where 10% (v/v) Alamar Blue was added to micro-channels and incubated for 4 hours. The resulting solution was removed from the culture plate and placed into the microplate reader, whose excitation and emission wavelengths were 535 nm and 590 nm, respectively. This study was conducted for 14 days. The results of this study are shown in Figure 9.12, where the cells in the micro-channels showed a continuous upregulation of cell proliferation during the 14-days investigation. Data gathered from the preliminary study showed an upregulation and then a decline in proliferation after day 7. Data gathered in this study did not show the same trend. In comparison to the 7F2 cells used in the preliminary study, the MDA-MB-231 cells grow at a slower rate, hence the slow proliferation rate up to day 7. The MDA-MB-231 cells continued to proliferate for the remainder of the study because there was sufficient room for the cells in the micro-channels to grow. This was not the case for the preliminary investigation: the 7F2 cells grew at a fast rate, and at day 7 of the study they ran out of room to grow, hence the decline of cell proliferation at the end of the 14-day study.

9.4.2.2 Cytotoxicity analysis

The MarkerGene^{TM} Live:Dead/Cytoxicity Assay Kit was used to provide qualitative data of cells in the micro-channels. Manufacturers' protocols were followed

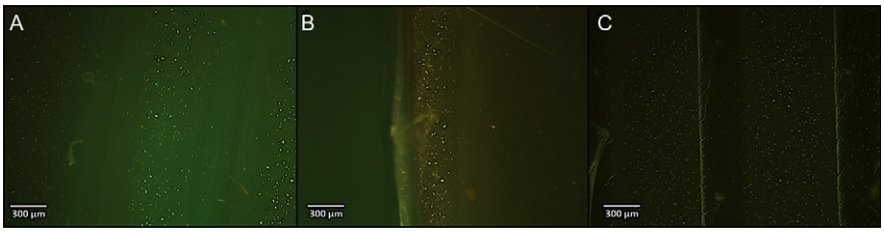

FIGURE 9.13

Live: Dead characterization of microfluidic chip of the MDA-MB-231 cell line on (A) day 7, (B) day 10, and (C) day 14.

to create the working live:dead solution from the propidium iodide (PI) solution and the carboxyfluorescein di-acetate (CFDA) solution. The carboxyfluorescein dye is retained in live cells, producing a green fluorescence, while cells with damaged membranes allow the entrance of PI, which undergoes a fluorescence enhancement upon binding to nucleic acids, promoting a red fluorescence in dead cells. Qualitative data were collected from the microfluidic cell-laden constructs on days 7, 10, and 14 after cells were printed in the channels. Figure 9.13 illustrates live (green) and dead (red) cells in the micro-channels of the construct. As seen in Figure 9.13, there are live (green glow) cells in the channels actively growing throughout the 14-day span.

9.4.2.3 Cell morphology

The micro-structural form of the micro-channels and cell morphology were evaluated using an FEI/Philips XL-30 Field Emission Environmental Scanning Electron Microscope (SEM). Images taken by SEM used a beam intensity of 2 KV and gaseous secondary electron detectors of 1.3 Torr. Before chips were characterized for architectural integrity and cell morphology, appropriate preparation was conducted by sectioning the lid of the enclosure. Sectioned samples were submerged in glutaraldehyde (GTA) (Sigma-Aldrich, St. Louis, MO) for 2 hours, followed by a dehydration process of submerging the GTA treated samples in 70%, 80%, 90%, 95%, and 100% ethanol for 10 minutes, respectively. Following the dehydration process, samples were placed under the culture hood for 1 hour to dry and then refrigerated overnight. Prior to SEM, samples were coated with platinum for enhanced visibility. As seen in Figure 9.14, channels are 300 μm wide and are uniform. Cells are attached in the channels and showed signs of proliferation. The morphology of the cells in the micro-channels is completely different from the morphology of cells in a two-dimensional culture. This may be due in part to the microfluidic environment [31–33].

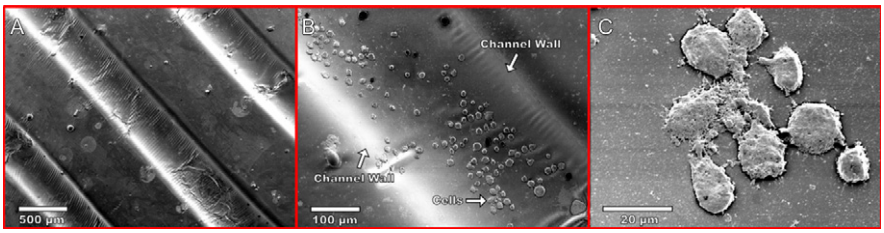

FIGURE 9.14

Scanning electron microscopy images showing (A) channel uniformity and orientation in the chip, (B) cell in the channel, and (C) close-up view of cells in the channel.

CONCLUSION

The DMM system has the capability to develop a biological microfluidic system. Chips fabricated with the DMM system have demonstrated their potential to promote cell attachment and proliferation. This preliminary investigation gives way for complex micro-architectural design for biological applications. The incorporation of a three-dimensional cell printer provided the added capabilities for precise spatial control of cells in the channels. Spatial orientation of cells will benefit the fabrication of complex future models; these models will be fabricated by a layer-by-layer technique. Additionally, the DMM system provides an economical fabrication technique to produce biological tissue arrays. The data presented show that the preliminary approach of developing a micro-platform to host cancerous cells is possible. The difference in cell morphology (two-dimensional vs. microfluidic) demonstrates that the micro-environment has a great influence on the cancer cells. A three-dimensional cancer model will closely mimic the in vivo conditions, thus providing researchers with an additional method of characterization pharmaceuticals.

References

[1] Starly B. Biomimetic design and fabrication of tissue engineered scaffolds using computer aided tissue engineering. Philadelphia, PA, USA: Drexel University; 2006 [Ph.D. Dissertation, Mechanical Engineering and Mechanics].

[2] Shor L. Novel fabrication development for the application of polycaprolactone and composite polycaprolactone/hydroxyapotote scaffolds for bone tissue engineering. Philadelphia, PA, USA: Drexel University; 2008 [Ph.D. Dissertation, Mechanical Engineering and Mechanics].

[3] Huang GY, Zhou LH, Zhang QC, Chen YM, Sun W, et al. Microfluidic hydrogels for tissue engineering. Biofabrication 2011;3:012001.

[4] Jo BH, Van Lerberghe LM, Motsegood KM, Beebe DJ. Three-dimensional microchannel fabrication in polydimethylsiloxane (PDMS) elastomer. J Microelectromech Syst 2000;9:76–81.
[5] Ho CM, Tai YC. Micro-electro-mechanical-systems (MEMS) and fluid flows. Annu Rev Fluid Mech 1998;30:579–612.
[6] Spearing SM. Materials issues in microelectromechanical systems (MEMS). Acta Mater 2000;48:179–96.
[7] The Organ and Transplantation Network. Available: <http://www.ustransplant.org>; 2004.
[8] Parnes LS, Sun AH, Freeman DJ. Corticosteroid pharmacokinetics in the inner ear fluids: an animal study followed by clinical application. Laryngoscope 1999;109:1–17.
[9] Elliott NT, Yuan F. A review of three-dimensional in vitro tissue models for drug discovery and transport studies. J Pharm Sci 2011;100:59–74.
[10] Zhang X, Wang W, Yu W, Xie Y, Zhang X, et al. Development of an in vitro multicellular tumor spheroid model using microencapsulation and its application in anticancer drug screening and testing. Biotechnol Prog 2005;21:1289–96.
[11] Hassan SB, de la Torre M, Nygren P, Karlsson MO, Larsson R, et al. A hollow fiber model for in vitro studies of cytotoxic compounds: activity of the cyanoguanidine CHS 828. Anticancer Drugs 2001;12:33–42.
[12] Cowan DS, Hicks KO, Wilson WR. Multicellular membranes as an in vitro model for extravascular diffusion in tumours. Br J Cancer Suppl 1996;27:S28–31.
[13] Casciari JJ, Hollingshead MG, Alley MC, Mayo JG, Malspeis L, et al. Growth and chemotherapeutic response of cells in a hollow-fiber in-vitro solid tumor-model. J Natl Cancer Inst 21 1994;86:1846–52.
[14] Friedrich MJ. Studying cancer in 3 dimensions—3-D models foster new insights into tumorigenesis. JAMA 2003;290:1977–9.
[15] Xiang D, Arnold MA. Solid-state digital micro-mirror array spectrometer for Hadamard transform measurements of glucose and lactate in aqueous solutions. Appl Spectrosc 2011;65:1170–80.
[16] Adeyemi AA, Barakat N, Darcie TE. Applications of digital micro-mirror devices to digital optical microscope dynamic range enhancement. Opt Express 2009;17:1831–43.
[17] Shin W, Yu BA, Lee YL, Yu TJ, Eom TJ, et al. Tunable Q-switched erbium-doped fiber laser based on digital micro-mirror array. Opt Express 2006;14:5356–64.
[18] Lu Y, Mapili G, Suhali G, Chen S, Roy K. A digital micro-mirror device-based system for the microfabrication of complex, spatially patterned tissue engineering scaffolds. J Biomed Mater Res A 2006;77:396–405.
[19] Gauvin R, Chen YC, Lee JW, Soman P, Zorlutuna P, et al. Microfabrication of complex porous tissue engineering scaffolds using 3D projection stereolithography. Biomaterials 2012;33:3824–34.
[20] Catros S, Guillemot F, Nandakumar A, Ziane S, Moroni L, et al. Layer-by-layer tissue microfabrication supports cell proliferation in vitro and in vivo. Tissue Eng Part C Methods 2012;18:62–70.
[21] Andersson H, van den Berg A. Microfabrication and microfluidics for tissue engineering: state of the art and future opportunities. Lab Chip 2004;4:98–103.
[22] Starly B, Sun W. Internal scaffold architecture designs using Lindenmayer systems. J Comput Aided Des Appl 2007;4:395–403.

[23] Nederman T, Acker H, Carlsson J. Penetration of substances into tumor tissue: a methodological study with microelectrodes and cellular spheroids. In Vitro 1983;19:479–88.
[24] Chang R, Sun W. Biofabrication of three-dimensional liver cell-embedded tissue constructs for in vitro drug metabolism models. LAP Lambert Academic Publishing; 2009.
[25] Sun W, Darling A, Starly B, Nam J. Computer-aided tissue engineering: overview, scope and challenges. Biotechnol Appl Biochem 2004;39:29–47.
[26] Sun W, Lal P. Recent development on computer aided tissue engineering–a review. Comput Methods Programs Biomed 2002;67:85–103.
[27] Guijt RM, Breadmore MC. Maskless photolithography using UV LEDs. Lab Chip 2008;8:1402–4.
[28] Hamid Q, Snyder J, Wang C, Timmer M, Hammer J, et al. Fabrication of three-dimensional scaffolds using precision extrusion deposition with an assisted cooling device. Biofabrication 2011;3:034109.
[29] Shor L, Guceri S, Chang R, Gordon J, Kang Q, et al. Precision extruding deposition (PED) fabrication of polycaprolactone (PCL) scaffolds for bone tissue engineering. Biofabrication 2009;1.
[30] Yan KC, Nair K, Sun W. Three dimensional multi-scale modelling and analysis of cell damage in cell-encapsulated alginate constructs. J Biomech 2010;43:1031–8.
[31] Hung PJ, Lee PJ, Sabounchi P, Lin R, Lee LP. Continuous perfusion microfluidic cell culture array for high-throughput cell-based assays. Biotechnol Bioeng 2005;89:1–8.
[32] Tourovskaia A, Figueroa-Masot X, Folch A. Differentiation-on-a-chip: a microfluidic platform for long-term cell culture studies. Lab Chip 2005;5:14–9.
[33] Kim MS, Yeon JH, Park JK. A microfluidic platform for 3-dimensional cell culture and cell-based assays. Biomed Microdevices 2007;9:25–34.